

Lung Ultrasound to Quantitatively Evaluate Extravascular Lung Water Content and its Clinical Significance

Guo Guo (✉ guoapple2006@163.com)

5th Medical Center of Chinese PLA General Hospital <https://orcid.org/0000-0003-1657-9638>

Xue-Feng Zhang

5th Medical Center of Chinese PLA General Hospital

Jing Liu

Beijing Chaoyang District Maternal and Child Healthcare Hospital

Hai-Feng Zong

Shenzhen Maternity&Child Healthcare Hospital

Research

Keywords: lung ultrasound, extravascular lung water, B-line, pulmonary edema

Posted Date: March 25th, 2020

DOI: <https://doi.org/10.21203/rs.3.rs-19227/v1>

License:  This work is licensed under a Creative Commons Attribution 4.0 International License.

[Read Full License](#)

Version of Record: A version of this preprint was published at The Journal of Maternal-Fetal & Neonatal Medicine on September 16th, 2020. See the published version at <https://doi.org/10.1080/14767058.2020.1812057>.

Abstract

Background: B-line assessment with lung ultrasound (LUS) has recently been proposed as a reliable, noninvasive semiquantitative tool for evaluating extravascular lung water (EVLW). Currently, there has been no easy quantitative method to evaluate EVLW by LUS. To establish a simple, accurate and clinically operable method for quantitative assessment of EVLW using LUS. **Methods:** Forty-five New Zealand rabbits were randomized into 9 groups (n=5). After anesthesia, each group of rabbits was injected with different amounts of warm sterile NS (0 ml/kg, 2 ml/kg, 4 ml/kg, 6 ml/kg, 8 ml/kg, 10 ml/kg, 15 ml/kg, 20 ml/kg, 30 ml/kg) via the endotracheal tube. Each rabbit was examined by LUS before and after NS injection. At the same time, the spontaneous respiratory rate (RR, breaths per minute), heart rate (HR, bpm) and arterial blood gas (ABG) of the rabbits were recorded. Then, both lungs were dissected to obtain the wet and dry weight and conduct a complete histological examination. **Results:** Injecting NS into the lungs through a tracheal tube can successfully establish a rabbit model with increased EVLW. When the NS injection volume is 2~6 ml/kg, comet-tail artifacts and B-lines are the main patterns found on LUS; as additional NS is injected into the lungs, the rabbits' RR gradually increases, while their HR gradually decreases. Confluent B-lines grow gradually but significantly, reaching a dominant position when the NS injection volume reaches 6~8 ml/kg and predominating almost entirely when the NS injection volume is 8~15 ml/kg; at that time, rabbits' RRs and HRs decrease sharply, and the ABG indicated type I respiratory failure (RF). Compact B-lines occur and predominate almost entirely when the NS injection volume reaches 10 ml/kg and 15~20 ml/kg, respectively. At that time, rabbits begin to enter cardiac and respiratory arrest, and ABG shows type II RF and metabolic acidosis (MA). **Conclusion:** LUS can estimate EVLW content based on the type of B-line. We can give clinical treatment depending on the type of LUS B-line.

Background

Extravascular lung water (EVLW) is the amount of fluid in the alveoli and interstitium. EVLW accumulation impairs respiratory gas exchange, resulting in respiratory distress, with subsequent organ dysfunction and increased mortality¹. Simple, accurate, rapid, and quantitative assessment of EVLW can help clinicians assess the extent of lung injury, select clinical treatments, and assess prognosis. Currently, several techniques exist to evaluate EVLW, but all have limitations. For example, transpulmonary thermodilution (TPTD) is the current reference standard, but it requires specialized equipment and is costly and invasive^{2,3}. Traditionally, chest X-ray has been used to evaluate EVLW; however, it has a poor correlation with EVLW changes and is often affected by subjective factors⁴.

Recently, lung ultrasound (LUS) has been frequently performed to evaluate EVLW in patients with respiratory or cardiovascular diseases⁵⁻¹⁰. Several studies have demonstrated⁵⁻¹⁰ a positive correlation between LUS B-line scores and EVLW¹¹⁻¹⁶. However, all these studies compared LUS results with EVLW as measured by TPTD or chest X-ray. For a more direct assessment, a tight correlation between B-lines and EVLW was confirmed by measuring the wet-to-dry ratio of postmortem lung tissue in a pig model¹⁷.

All these studies have showed that there is a clear relationship, semiquantitative or otherwise, between LUS results and EVLW.

The complexity of LUS B-line scores is not convenient for rapid clinical judgment, especially for critically ill patients. In addition, LUS B-line scores themselves can be compromised by a variety of factors, including subjective factors at the level of the operator¹⁸. Therefore, it is particularly important to establish a method for quantitatively evaluating EVLW in a simple, fast, accurate and reliable manner. In this study, we established an animal model of EVLW increase by injecting normal saline (NS) into the lungs via endotracheal tubes, established a method for quantitative assessment of EVLW by LUS, and explored the clinical intervention threshold of EVLW increase. We proposed a novel classification of B-line types and found that the type of B-line was related to the EVLW content.

Materials And Methods

Animal preparation

Forty-five male New Zealand rabbits weighing 2.6–3.5 kg (average 3.0 ± 0.3 kg) were divided into 9 groups, with 5 rabbits in each group. The animals were fasted for 12 hours, weighed, anesthetized (20% sodium pentobarbital, 20–40 mg/kg, ear vein injection), depilated and fixed on a rabbit surgery platform. A T-shaped incision was made in the trachea; then a tracheal tube (inner diameter 3.0 mm, with airbag) was inserted into the trachea to an insertion depth of 2 cm (Fig. 1). The respiratory rate and heart rate of each rabbit were recorded after tracheal intubation.

Rabbit model

Warm sterile NS was injected into the lungs of each rabbit via an endotracheal tube. The NS injection in each group was 0 ml/kg, 2 ml/kg, 4 ml/kg, 6 ml/kg, 8 ml/kg, 10 ml/kg, 15 ml/kg, 20 ml/kg, and 30 ml/kg. Half of the NS was injected in the left lateral position, and the other half was injected in the right lateral position. After NS injection, positive pressure ventilation was performed for 3–5 minutes to ensure that no water flowed back from the tracheal intubation. Then, the RR and HR of the rabbits were recorded.

Ventilation

After the injection of NS, mechanical ventilation was initiated using an animal respirator (SuperV, Laiyue, Shenzhen, China), with the following settings: Mode: volume-controlled. Parameters: fractional inspired oxygen (FiO_2) 21%, inspiratory/expiratory ratio 1:2, respiratory rates 20 breaths/min, tidal volume 8 mL/kg, positive end-expiratory pressure (PEEP) 4 cmH₂O.

LUS examination

Ultrasound examinations were performed with a commercially available portable device (EDAN ultrasound diagnostic system, China) with a 9–12 MHz linear probe in B-mode. Each lung was divided into 3 zones, for a total of 6 zones¹⁹. The area from the parasternal line to the anterior axillary line was

zone 1; the area from the anterior axillary line to the posterior axillary line was zone 2; and the area from the posterior axillary line to the paravertebral line was zone 3. Every zone included upper and lower parts, which were recorded as follows: the upper part of zone 1 of the left lung (L1/1), the lower part of zone 1 of the left lung (L1/2), etc. (Fig. 2). The scanning in zone 1 was in the supine position, zone 2 was in the lateral position, and zone 3 was in the prone position. Each area was scanned with a probe through the vertical gaps between ribs.

Arterial blood gas (ABG) analysis

The right/left inguinal connective tissue was separated to expose the femoral artery. Arterial blood specimens (1-1.5 ml each) were extracted with a 2 ml syringe moistened with heparin sodium saline. Then, the femoral artery was immediately ligated to prevent bleeding (Fig. 3). The specimen was tested with a portable blood gas analyzer (OPTI CCA-TS blood gas analyzer, China).

Measurement of lung water

The lungs were dissected free from the heart and great vessels, the trachea was separated at the carina, external liquid was removed by blotting, and the lungs were placed on a preweighed pan to obtain the wet weight. The lungs were then incubated in a dry atmosphere at 80 °C for 72 hours and reweighed to obtain the dry lung weight. The wet/dry ratio = wet lung weight/dry lung weight.

Lung ultrasonography terminology^{11,20}

Comet-tail artifacts and B-lines: Both comet-tail artifacts and B-lines arise from and are roughly vertical to the pleural line, synchronously moving with lung sliding. Those not spreading to the edge of the screen are called comet-tail artifacts, and those spreading to the edge of the screen without fading are known as B-lines. The width of the starting point of the B-lines from the pleural line does not exceed 1/2 of the intercostal space width are called of B-lines.

Confluent B-lines: The width of the starting point of the B-lines from the pleural line is wider than or equal to 1/2 of the intercostal space width, but the B-lines between different intercostal spaces are not fused, and rib acoustic shadows still exist.

Compact B-lines: When the probe is used to scan perpendicular to the ribs, which causes the rib acoustic shadows to disappear substantially throughout the scanning area, the pattern is called a compact B-line (Fig. 6).

Total B-lines and B-lines in different zones

Total B-lines: According to the LUS image, the sum of the comet-tail artifacts and B-lines in the six regions of the lungs after NS injection were calculated.

B-lines in different zones: According to the LUS image, calculate the number of comet-tail artifacts and B-lines in each area of the zone 1, zone 2, and zone 3 regions of both lungs after NS injection.

Histological Examination

We selected visible lesions of the rabbit lungs with the naked eye to take samples, slice, stain and observe under the microscope.

Statistical analysis

All data are presented as the mean \pm SD. Statistical analysis was performed using the SPSS (version 19.0, SPSS) software package. Differences between baseline and each experimental point were tested using one-way analysis of variance (ANOVA). The correlation between the amount of NS injected into the lung and the lung wet/dry ratio was linearly correlated. The difference between comet-tail artifacts, B-lines, confluent B-lines and compact B-lines was analyzed by systematic clustering method. For all the statistical analyses, significance was accepted at $P < 0.05$.

Results

The relationship between NS injection volume and lung wet weight, lung dry weight and wet/dry ratio

The results of NS injection volume, body weight (BW), lung wet weight (WW), lung dry weight (DW) and lung wet/dry ratios (W/D) are shown in Table 1. ANOVA showed that there was no difference in lung dry weight ($P > 0.05$), but the difference between the BW of each group was statistically significant ($P < 0.05$). As the amount of NS injection increases, the wet weight of the lung and the wet/dry ratio gradually increase. A statistically significant linear correlation was found between NS injection volume and wet/dry ratio: Y (wet/dry ratio) = $0.5865X$ (NS injection volume) + 5.4427 , $R^2 = 0.96601$ (Fig. 7).

Table 1

The results of NS injection volume and lung wet/dry ratio in rabbit lungs ($x \pm s$)

Group (n=)	NS injection volume(ml/kg)	BW(kg)	WW(g)	DW(g)	W/D ratio
1(5)	0	3.06 ± 0.18	10.93 ± 0.42	2.41 ± 0.35	4.59 ± 0.56
2(5)	2	3.38 ± 0.18	15.79 ± 2.20	2.43 ± 0.46	6.54 ± 0.52
3(5)	4	3.06 ± 0.35	19.38 ± 2.50	2.45 ± 0.34	7.93 ± 0.63
4(5)	6	3.02 ± 0.30	22.63 ± 2.62	2.28 ± 0.33	9.95 ± 0.54
5(5)	8	2.96 ± 0.11	25.89 ± 1.75	2.43 ± 0.12	10.67 ± 0.78
6(5)	10	3.06 ± 0.21	28.46 ± 2.84	2.52 ± 0.24	11.31 ± 0.67
7(5)	15	2.92 ± 0.08	32.11 ± 0.39	2.54 ± 0.14	12.68 ± 0.62
8(5)	20	2.80 ± 0.16	42.80 ± 2.96	2.33 ± 0.17	18.35 ± 0.83
9(5)	30	2.76 ± 0.09	63.89 ± 0.55	2.82 ± 0.06	22.68 ± 0.61

Histological examination

The pathological results of the lung tissue sections of the lesions visible to the naked eye after the NS injection of the rabbits in Groups 2–9 are shown in Fig. 8. Alveolar epithelial cells are flat, and local alveolar excessive expansion, rupture, and fuse into alveolar sacs.

The relationship between NS injection volume and respiratory rates, heart rates and blood gas results

The statistical results of the NS injection volume to the lungs of the rabbits and the respiratory rates and heart rates after NS injection are shown in Table 2. When the NS injection volume is ≤ 10 ml/kg, the respiratory rate gradually increases to 140 bpm, and the heart rate gradually decreases to approximately 150–200 bpm with the increase in NS injection in the lungs; when 10 ml/kg $<$ the NS injection volume ≤ 15 ml/kg, the respiratory rates and heart rates drop sharply. Respiratory and cardiac arrest occur when the NS injection volume is ≥ 15 ml/kg, as shown in Figs. 8 and 9. When the NS injection volume is < 10 ml/kg, the ABG is normal or shows metabolic acidosis (MA). When the NS injection volume is 2 ~ 6 ml/kg, the ABG shows normal or mild MA. When the NS injection volume reaches 8 ml/kg, the rabbits start to develop type I respiratory failure (RF). When the NS injection volume reaches 10 ml/kg, ABG shows type II RF and MA.

Table 2
Respiratory rate, heart rate, and ABG results after different volumes of NS injection

Group(n=)	NS injection volume(ml/kg)	RR (bpm)	HR (bpm)	ABG
1(5)	0	30.4 ± 5.2	271.6 ± 9.3	Normal
2(5)	2	57.6 ± 16.7	259.2 ± 32.7	Normal
3(5)	4	72.4 ± 22.8	241.6 ± 19.7	MA
4(5)	6	119.6 ± 27.9	241 ± 19.0	MA
5(5)	8	135.0 ± 14.2	245 ± 12.2	Type I RF
6(5)	10	139.4 ± 26.1	179.2 ± 19.2	Type I/II RF with MA
7(5)	15	0 ± 0	12 ± 26.8	Type II RF with MA
8(5)	20	0 ± 0	0 ± 0	Type II RF with MA
9(5)	30	0 ± 0	0 ± 0	Type II RF with MA

MA: metabolic acidosis, RF: respiratory failure, ABG: arterial blood gas.

LUS B-line results and cluster analysis results

The results concerning comet-tail artifacts, B-lines, confluent B-lines and compact B-lines in Groups 1–9 are shown in Table 3. Systematic cluster analysis was performed using their mean values. The ice and tree diagrams shown in Figs. 11 and 12 clearly show the entire clustering process. First, it is assumed that the four samples of the comet-tail artifact, B-line, confluent B-line and compact B-line become one type; after the first cluster combination, the comet-tail artifact and B-line are clustered into one type, and the confluent B-line is another. For the second category, the compact B-line is clustered into the third category. Therefore, we come to that the similarity of comet-tail artifacts and B-lines is high and less separable, but it is more separable from confluent B-lines and compact B-lines.

Table 3
 Ultrasound B-line statistical results of rabbit lungs after NS injection

Group(n=)	Water(ml/kg)	Comet-tail artifact (n)	B-line (n)	Confluent B-line (n)	Compact B-line (n)
1(5)	0	0 ± 0	0 ± 0	0 ± 0	0 ± 0
2(5)	2	2.4 ± 1.8	5.6 ± 4.6	0 ± 0	0 ± 0
3(5)	4	1.2 ± 1.3	6.8 ± 1.8	3.4 ± 1.3	0 ± 0
4(5)	6	1.2 ± 1.1	11.4 ± 2.5	10.6 ± 6.8	0 ± 0
5(5)	8	0 ± 0	7.6 ± 2.7	17.2 ± 2.8	0 ± 0
6(5)	10	0 ± 0	4.4 ± 1.9	19.4 ± 9.2	5.8 ± 8.6
7(5)	15	0 ± 0	1.8 ± 2.9	22.2 ± 5.0	6.4 ± 2.6
8(5)	20	0 ± 0	3 ± 2.6	14.3 ± 3.5	21.0 ± 2.6
9(5)	30	0 ± 0	0 ± 0	4.6 ± 1.9	37.2 ± 2.6

Relationship between total LUS B-lines and NS injection volume

According to the scatter plot, the type of B-line and its quantity are constantly changing with NS injection volume. The main changes are as follows:

- a. When the NS injection volume is 2-6 ml/kg, comet-tail artifacts and B-lines predominate on LUS.
- b. When the NS injection volume >4 ml/kg, confluent B-lines begin to occur in the LUS. When the NS injection volume reaches 6~8 ml/kg, confluent B-lines increase significantly and gradually become dominant. When the NS injection volume is 8~15 ml/kg, confluent B-lines predominate almost entirely.
- c. When the NS injection volume reaches 10 ml/kg, compact B-lines occur in the LUS. As the amount of NS injection increases, compact B-lines gradually increases. When the NS injection volume reaches 15~20 ml/kg, LUS is mainly performed by compact B-lines (Fig. 13).

In summary, the type of B-lines in the LUS can be used to quantitatively estimate the amount of water in the lungs. There is also a clear correlation between LUS and clinical manifestations. Therefore, we can guide clinical treatment based on LUS performance.

Relationship between B-lines in different zones and NS injection volume

The trend of the relationship between B-lines in different zones and NS injection volume is consistent with that between total B-lines and NS injection volume, but the advantage of zone1 is more obvious when the NS injection volume is ≤ 6 ml/kg, mainly based on comet-tail signs and B-lines. When the NS injection volume is 8 ~ 15 ml/kg, the B-lines in any zone can be used to estimate the total B-lines. However, when the NS injection volume is 15 ~ 20 ml/kg, zone 2 and zone 3 B-lines are more consistent with the total B-lines.

Discussion

Alveolar lavage, the pulmonary surfactant washout method, is one of the most commonly used methods for establishing an animal model of acute lung injury (ALI)²¹. To acquire a uniform degree of injury in the whole lung, some researchers shift the animals from the supine to the prone position or vice versa between the lavages^{22,23}. We borrowed the same method, for the purpose of obtaining an animal model with a consistent degree of intrapulmonary lesions, the rabbits were changed in position during the intrapulmonary injection. In addition, to obtain a rabbit model with different lung water contents, we did not extract NS injected into the lungs but injected different amounts of NS into the lungs as needed. Finally, we found that there was a linear positive correlation between NS injection and the lung wet/dry ratio. Kuckelt and Huber observed that the pathological changes in the lung tissue of the ALI model established by alveolar lavage were mainly characterized by excessive expansion and atelectasis of alveoli in different areas, and no intrapulmonary hemorrhage or cell necrosis was observed^{24,25}. We found alveolar sacs formed by fusion of alveolar rupture was the main pathological change on rabbit models, and no hemorrhage or alveolar septal thickening were observed.

Monitoring EVLW as a variable is increasingly being used to diagnose and treat critically ill patients with ALI^{26,27}. The current gold standard is the gravimetric method, which directly compares the wet weight and dry weight of the lung to determine the water content in the lungs. However, this method is invasive, and feasible only at the time of autopsy²⁸⁻³⁰. The most common method used in the clinic is the transpulmonary indicator dilution technique, in which transpulmonary double indicator dilution (TPDD) has been considered to be the clinical gold standard verified by gravimetry³¹. This technique is a reliable bedside method to measure EVLW but may be influenced by regional lung perfusion, type of lung injury, and amount of EVLW³²⁻³⁴. Chest computed tomography is the most accurate tool to visualize lung parenchyma; however, it uses ionizing radiation and requires transportation of the patient outside the intensive care unit, often with mechanical ventilation and complex cardiovascular monitoring³⁵.

Compared to the techniques described above, LUS is a simple, bedside, noninvasive, real-time, nonradioactive new technique that has been developed in many intensive care unit(ICU) wards. Our research group has conducted clinical research on LUS for a long time and published a series of articles on LUS diagnosis of pulmonary edema and wet lungs of newborns³⁶⁻³⁹. We found that LUS has high sensitivity and specificity in the diagnosis of pulmonary edema and wet lungs of newborns. Our results

have been recognized internationally, which has laid the foundation for our LUS examination of the EVLW augmented rabbit model.

In addition, several studies were published demonstrating a positive correlation between B-line scores and EVLW. Volpicelli and colleagues measured EVLW in 32 ventilated general ICU patients with TPTD and found that the absence of B-lines (A-line pattern) was associated with low levels of EVLW (10 mL/kg or less)¹². Another study reported that the sensitivity and specificity of a positive B-line score for the detection of EVLW of > 500 mL were 90% and 86%, respectively¹³. In addition, studies have verified the close correlation between the B-line and EVLW by measuring the wet/dry ratio of lung tissue in pig models¹⁴. Since 2004, Jambrik has found that pulmonary ultrasound can be used to detect EVLW⁴⁰. Later, there were an increasing number of studies on the relationship between the LUS B-line score and EVLW. However, the current B-line scoring method mostly divides the lung into several subregions and then scores according to the total number of B-lines in each region. When the lesion is serious, the B-line can reach dozens, and the calculation process is cumbersome^{14,41,42}. One of the main values of our experiment is to find that the amount of EVLW is related not only to the number of B-lines but also to the type of B-lines. We found through cluster analysis that the comet-tail artifacts and B-line observed in the experiment are not much different and can be classified into the same category, which is common when the NS injection volume is below 6 ml/kg. Combined with our experimental results, when the comet-tail artifacts and B-lines are mainly in the lung field, the the NS injection volume is approximately 2 ~ 6 ml/kg; when the lung field is dominated by the confluent B-line, the NS injection volume is approximately 8–15 ml/kg; when the compact B-line is dominant, the NS injection volume is above 20 ml/kg. Combined with the classification of LUS B-lines, it is not necessary to count the number of B-lines in detail as reported in the past, and the EVLW can be semiquantitatively determined from the B-line type, which provides great convenience for the clinical application of LUS to assess lung water content.

We used a parallel experimental method to not only study the relationship between gravity measurement and lung water severity but also observe changes in rabbit breathing, heart rate and ABG after injection of different NS volumes. When the NS injection volume is below 10 ml/kg, breathing gradually increases, the heart rate gradually slows, and ABG is mainly caused by simple MA or hypoxemia. When the NS injection volume was between 10 ml/kg and 15 ml/kg, the breathing and heart rate decreased rapidly. When the NS injection is more than 15 ml/kg, breathing and cardiac arrest will occur immediately after the water injection. The ABG will also be characterized by MA combined with type I or type II RF. Combined with LUS quantitative assessment of EVLW, when the lung field is dominated by comet-tail artifacts or B-lines, the clinical manifestations of increased breathing and slow heart rate are basically within the compensable range. When the lung field is dominated by the confluent B-line, the breathing and heart rate drop sharply. If clinical support is not given, the clinical symptoms may deteriorate sharply. When the compact B-line is predominant in the lung field, respiratory support is a must, and breathing and cardiac arrest may occur at any time. Through experimental NS injection into the lungs, LUS performance and assessment of respiration and heart rate, LUS quantitative assessment of EVLW to guide clinical treatment is possible, but due to the complexity of clinical cases and the different tolerances of humans

and rabbits to damage, further rigorously designed animal experiments and related clinical trials are needed to further establish the relationship between LUS performance and clinical patient performance and treatment options.

In addition, each clinical examination must have its safety issues considered before it is carried out. The benefits of LUS implementation are obvious, but there is also a potential for ultrasound lung injuries^{43,44}. Although ultrasound can cause pulmonary capillary hemorrhage in mammals such as rats, it occurs above the threshold of exposure levels and is also related to physiological conditions, such as changes caused by different anesthesia methods⁴⁵. To date, there have been no reports of major medical problems caused by LUS; therefore, it is currently considered safe.

Conclusions

LUS can roughly estimate EVLW content based on the type of B-line. When the LUS mainly features comet-tail artifacts and B-lines, the rabbits do not have obvious clinical syndromes and do not need clinical treatment. When the LUS is predominated by confluent B-lines, the EVLW is approximately 8 ~ 15 ml/kg, and the rabbits start to show RF, with a possible need for clinical intervention. Beyond that point, additional EVLW poses a threat to life.

Abbreviations

Arterial Blood Gas-ABG

One-way Analysis of Variance -ANOVA

Acute Lung Injury -ALI

Body Weight -BW

Dry Weight -DW

Extravascular Lung Water -EVLW

Heart Rate -HR

Lung Ultrasound -LUS

Metabolic Acidosis -MA

Normal Saline -NS

Positive End-expiratory Pressure -PEEP

Respiratory Rate -RR

Respiratory Failure -RF

Transpulmonary Thermodilution –TPTD

Transpulmonary Double Indicator Dilution -TPDD

Wet Weight –WW

Wet/Dry ratios -W/D

Declarations

Ethics approval and consent to participate

This experiment was approved by the Animal Ethics Committee of 302 Military Hospital(Approval ID:IACUC-2018-016).

Consent for publication

Not applicable.

Availability of data and materials

All data generated or analysed during this study are included in this published article.

Competing interests

The authors declare that they have no competing interests.

Funding

The Clinical Research Special Fund of Wu Jieping Medical Foundation (320.6750.15072).

Authors' contributions

Jing L contributed substantially to the study design, and revised the draft manuscript. Guo G participated in the study design and complete the experiments, performed data analysis, and wrote the draft manuscript. Hai-feng Z participated in the experiments. Xue-feng Z provided the experimental site and revised the draft manuscript.

Acknowledgments

Not applicable.

References

1. Sherif A, Wolf BK, Benjamin S, Malcolm BF, Albert PJr. Assessment of pulmonary edema: principles and practice. *J Cardiothorac Vasc Anesth.* 2018; 32:901–14.
2. Rob MS, Daniel FMA. Acute respiratory distress syndrome. *Lancet.* 2016; 388:2416–30.
3. Takashi T, Shigeki K, Yasuhiro Y, et al. Validation of extravascular lung water measurement by single transpulmonary thermodilution: human autopsy study. *Crit Care.* 2010;14: R162.
4. Bruce DH, Thomas WF, Frederick GM, Caroline C, Diana FG, Norman EB. Evaluation of the portable chest roentgenogram for quantitating extravascular lung water in critically ill adults. *Chest.* 1985;88:649-52.
5. Luna G. Lung ultrasound: a new tool for the cardiologist. *Cardiovasc Ultrasound.* 2011;9:6.
6. Giovanni V, Mahmoud E, Michael B, et al. International evidence-based recommendations for point-of-care lung ultrasound. *Intensive Care Med.* 2012;38: 577–91.
7. Marcelo HM, Luna G, Roberto TSA, et al. Lung ultrasound for the evaluation of pulmonary congestion in outpatients: a comparison with clinical assessment, natriuretic peptides, and echocardiography. *JACC Cardiovasc Imaging.* 2013;6:1141–51.
8. Marcelo HM, Eugenio P, Luigi PB, et al. Pulmonary congestion evaluated by lung ultrasound predicts decompensation in heart failure outpatients. *Int J Cardiol.* 2017;240: 271-8.
9. Bataille B, Guillaume R, Pierre C, et al. Accuracy of ultrasound B-lines score and E/Ea ratio to estimate extravascular lung water and its variations in patients with acute respiratory distress syndrome. *J Clin Monit Comput.* 2015;29:169-76.
10. Giacomo B, Luna G, Antonio A, et al. Lung water assessment by lung ultrasonography in intensive care: a pilot study. *Intensive Care Med.* 2013;39:74–84.
11. Daniel AL, Gilbert AM. Relevance of lung ultrasound in the diagnosis of acute respiratory failure: the BLUE protocol. *Chest.* 2008;134:117–25.
12. Christian BL, Anja H, Stefan P, Søren M, Lars V, Henrik B. Prehospital lung ultrasound for the diagnosis of cardiogenic pulmonary edema: a pilot study. *Scand J Trauma Resusc Emerg Med.* 2016;24:96.
13. Krochmal-Mokrzan EM, Barker PM, Gatzky JT. Effects of hormones on potential difference and liquid balance across explants from proximal and distal fetal rat lung. *J Physiol.* 1993;463:647–65.
14. Giovanni V, Stefano S, Enrico B, et al. Lung ultrasound predicts well extravascular lung water but is of limited usefulness in the prediction of wedge pressure. *Anesthesiology.* 2014;121: 320-7.
15. Eustachio A, Tiziana B, Michele O, et al. “Ultrasound comet-tail images”: a marker of pulmonary edema: a comparative study with wedge pressure and extravascular lung water. *Chest.* 2005;127: 1690-5.

16. Philipp E, Sibylle R, Jens N, et al. Simplified lung ultrasound protocol shows excellent prediction of extravascular lung water in ventilated intensive care patients. *Crit Care*. 2015;19:36.
17. Zoltân, Luna G, Agnes A, et al. B-lines quantify the lung water content: a lung ultrasound versus lung gravimetry study in acute lung injury. *Ultrasound Med Biol*. 2010;36: 2004-10.
18. Jing L. The Lung Ultrasound Score Cannot Accurately Evaluate the Severity of Neonatal Lung Disease. *J Ultrasound Med*. 2019; doi:10.1002/jum.15176.
19. Division of Perinatology, Society of Pediatric, Chinese Medical Association, et al. Guideline on lung ultrasound to diagnose pulmonary diseases in newborn infants. *Chin J Contemp Pediatr*. 2019, 21: 105-13.
20. Jing L, Roberto C, Erich S, et al. Protocol and guidelines for point-of-care lung ultrasound in diagnosing neonatal pulmonary diseases based on international expert consensus. *J Vis Exp*. 2019;145:e58990.
21. Wang HM, Bodenstein M, Markstaller K. Overview of the pathology of three widely used animal models of acute lung injury. *Eur Surg Res*. 2008;40: 305-16.
22. Guido M, R Scott H, Marcos FVM, et al. Mechanism by which a sustained inflation can worsen oxygenation in acute lung injury. *Anesthesiology*. 2004;100: 323–30.
23. Carissa LBB, Andrew MH, Larry WT, Edward PI, Bela S, David WK, Brett AS, Kenneth RL. Relationship between dynamic respiratory mechanics and disease heterogeneity in sheep lavage injury. *Crit Care Med*. 2007;35: 870–8.
24. Kuckelt W, Dauberschmidt R, Bender V, et al. Experimental investigations in adult respiratory distress syndrome (ARDS). Repeated pulmonary lavage in LEWE-mini-pigs. I. Pulmonary mechanics, gas exchange, and pulmonary hemodynamics. *Exp Pathol*. 1981;20: 88–104.
25. Huber GL, Edmunds LH Jr, Finley TN. Acute effect of saline lung washing on pulmonary mechanics and morphology. *Surg Forum*. 1966;17:113–4.
26. Mathieu J, Serena S, Romain P, et al. Extravascular lung water is an independent prognostic factor in patients with acute respiratory distress syndrome. *Crit Care Med*. 2013;41:472–80.
27. Samir GS, Magdalena K, Konrad R, Andreas M-H. Prognostic value of extravascular lung water in critically ill patients. *Chest*. 2002;122:2080–6.
28. Pearce ML, Yamashita J, Beazell J. Measurement of pulmonary edema. *Circ Res*. 1965; 16:482-8.
29. Julien M, Flick MR, Hoeffel JM, et al. Accurate reference measurement for postmortem lung water. *J Appl Physiol Respir Environ Exerc Physiol*. 1984; 56:248–53.

30. Collins JC, Newman JH, Wickersham NE, et al. Relation of blood-free to blood-inclusive postmortem lung water measurements in sheep. *J Appl Physiol*. 1985;59:592–6.
31. Mihm FG, Feeley TW, Jamieson SW. Thermal dye double indicator dilution measurement of lung water in man: Comparison with gravimetric measurements. *Thorax*. 1987;42:72–6.
32. Schreiber T, Hüter L, Schwarzkopf K, et al. Lung perfusion affects preload assessment and lung water calculation with the transpulmonary double indicator method. *Intensive Care Med*. 2001;27:1814–8.
33. R Blaine E, Daniel GM, Christopher TL, et al. Redistribution of pulmonary blood flow impacts thermodilution-based extravascular lung water measurements in a model of acute lung injury. *Anesthesiology*. 2009;111:1065–74.
34. Frédéric M, Alexander S, Christian T. Factors in uencing the estimation of extravascular lung water by transpulmonary thermodilution in critically ill patients. *Crit Care Med*. 2005;33:1243–7.
35. Luciano G, Pietro C, Massimo C, et al. Lung recruitment in patients with the acute respiratory distress syndrome. *N Engl J Med*. 2006; 354:1775–86.
36. Shui-Wen C, Wei F, Jing L, Yan W. Routine application of lung ultrasonography in the neonatal intensive care unit. *Medicine(Baltimore)*. 2017;96:e5826.
37. Jing L, Xin-Xin C, Xiang-Wen L, Shui-Wen C, Yan W, Wei F. Lung Ultrasonography to Diagnose Transient Tachypnea of the Newborn. *Chest*. 2016;149:1269-75.
38. Jing L, Hai-Ying C, Xin-Ling W, Li-Jun X. The significance and the necessity of routinely performing lung ultrasound in the neonatal intensive care units. [J Matern Fetal Neonatal Med](#). 2016;29:4025-30.
39. Jing L. Lung ultrasonography for the diagnosis of neonatal lung disease. [J Matern Fetal Neonatal Med](#). 2014;27:856-61.
40. Zoltan J, Simonetta M, Vincenzo C, et al. Usefulness of ultrasound lung comets as a nonradiologic sign of extravascular lung water. *Am J Cardiol*. 2004;93:1265-70.
41. Kamal SA, Toshihiro O, Hiromichi N, et al. DireCt Lung Ultrasound Evaluation (CLUE): A novel technique for monitoring extravascular lung water in donor lungs. *J Heart Lung Transplant*. 2019;38:757-66.
42. Mohamed E, Mai AM, Ahmed AAM, et al. Effect of ultrafiltration on extravascular lung water assessed by lung ultrasound in children undergoing cardiac surgery: a randomized prospective study. *BMC Anesthesiol*. 2019;19: 93.

43. William DO Jr, Yan Y, Douglas GS, et al. Threshold estimation of ultrasound-induced lung hemorrhage in adult rabbits and comparison of thresholds in mice, rats, rabbits and pigs. *Ultrasound Med Biol.* 2006;32:1793–1804.

44. Douglas LM, Zhihong D, Chunyan D, Krishnan R. Does intravenous infusion influence diagnostic ultrasound-induced pulmonary capillary hemorrhage? *J Ultrasound Med.* 2018;37: 2021–8.

45. Douglas LM. Mechanisms for induction of pulmonary capillary hemorrhage by diagnostic ultrasound: review and consideration of acoustical radiation surface pressure. *Ultrasound Med Biol.* 2016,42:2743-57.

Figures

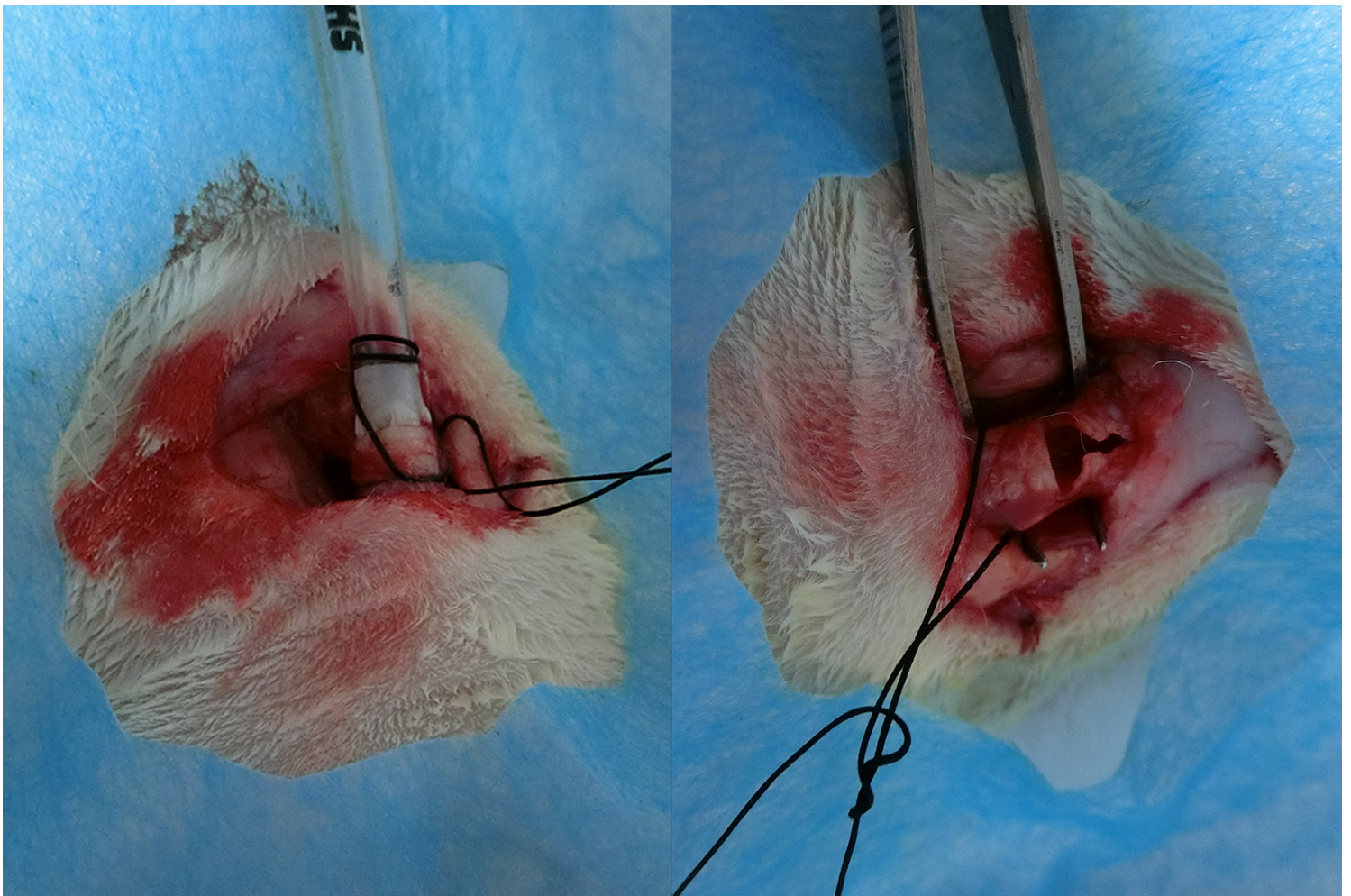


Figure 1

Tracheotomy and intubation

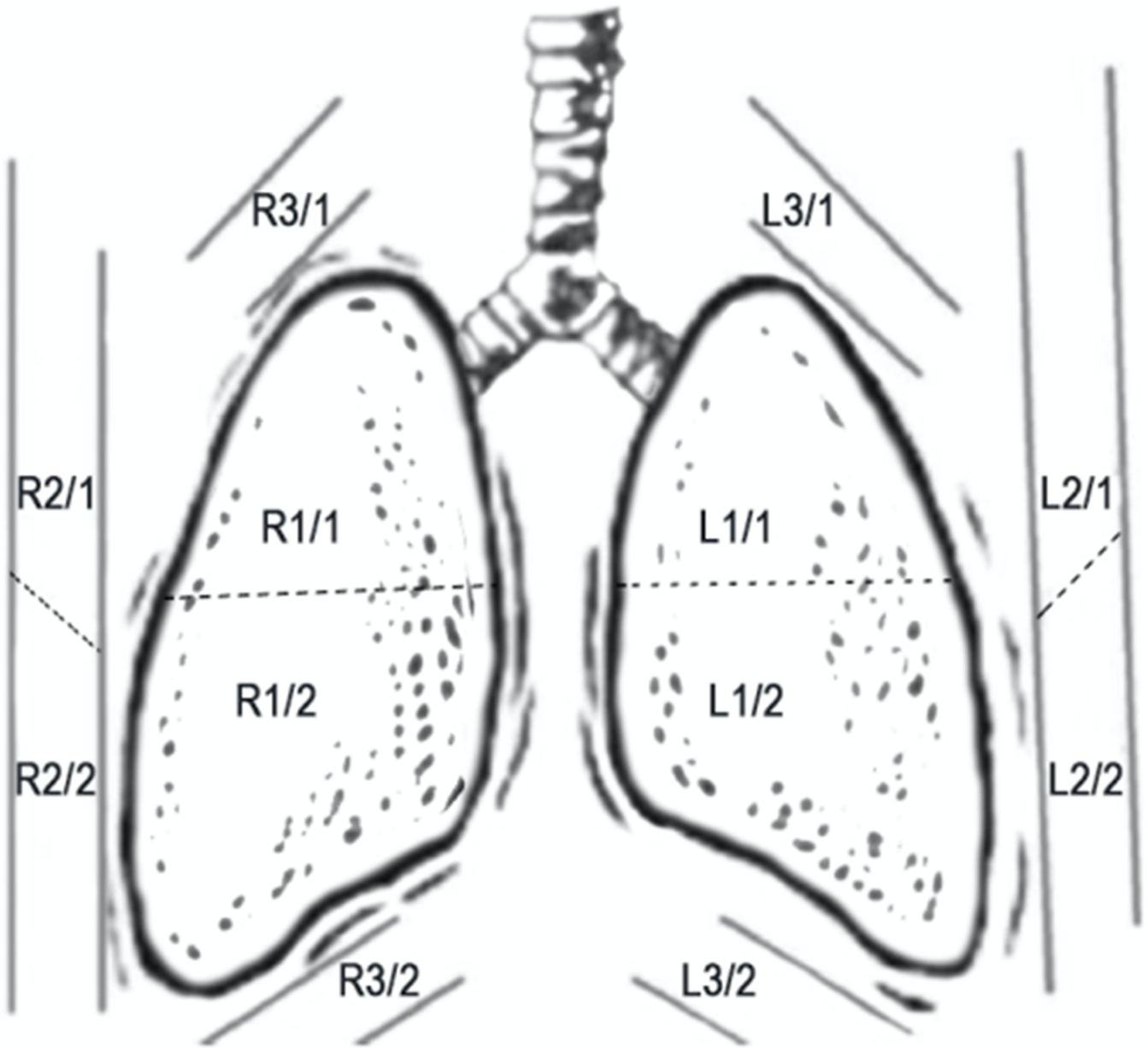


Figure 2

Anatomical partitions of the lungs

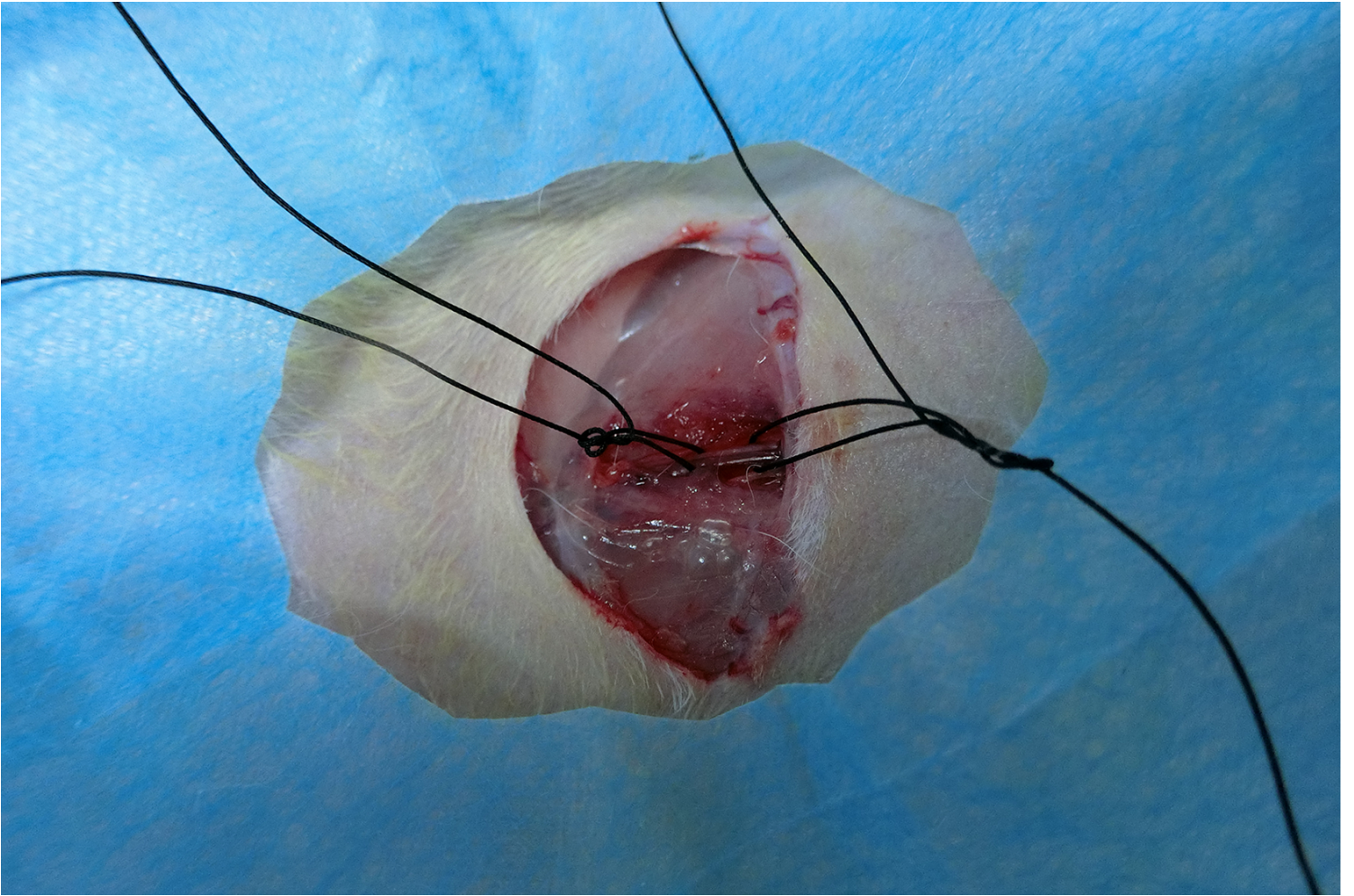


Figure 3

Arterial blood gas specimen collection



Figure 4

Wet lung tissue

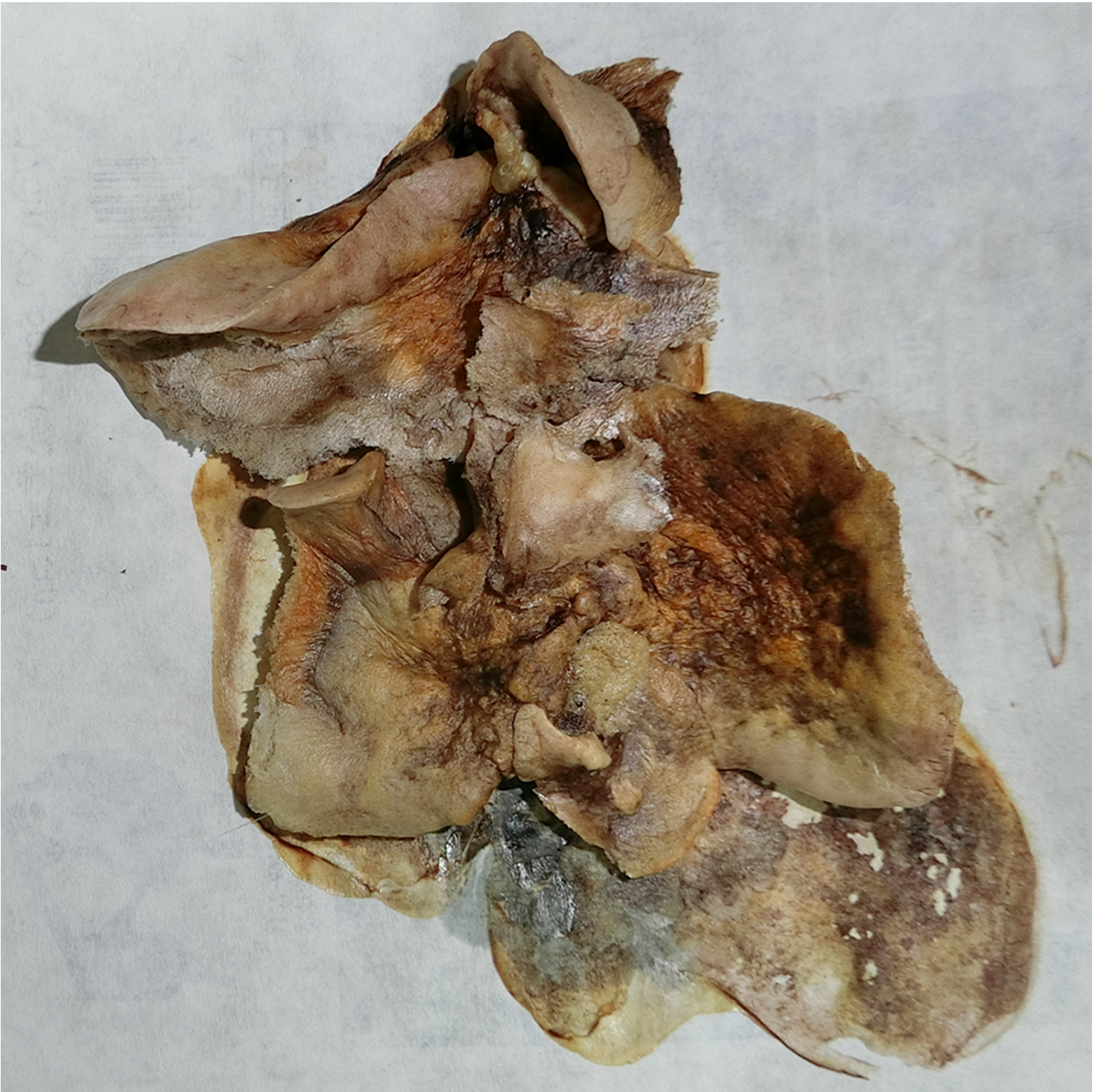


Figure 5

Dry lung tissue

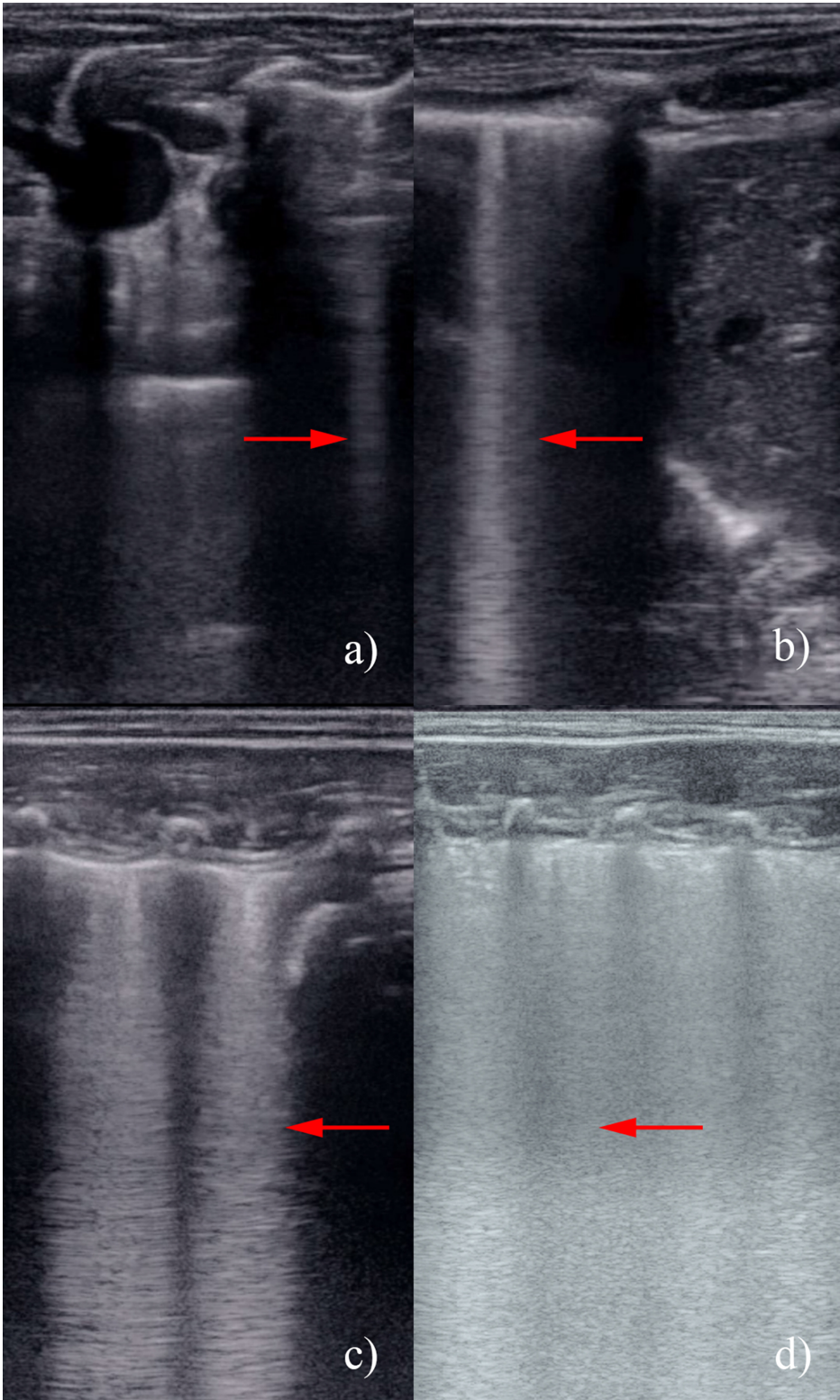


Figure 6

Classification of B-lines a) Comet-tail artifacts, b) B-line, c) Confluent B-line, d) Compact B-line

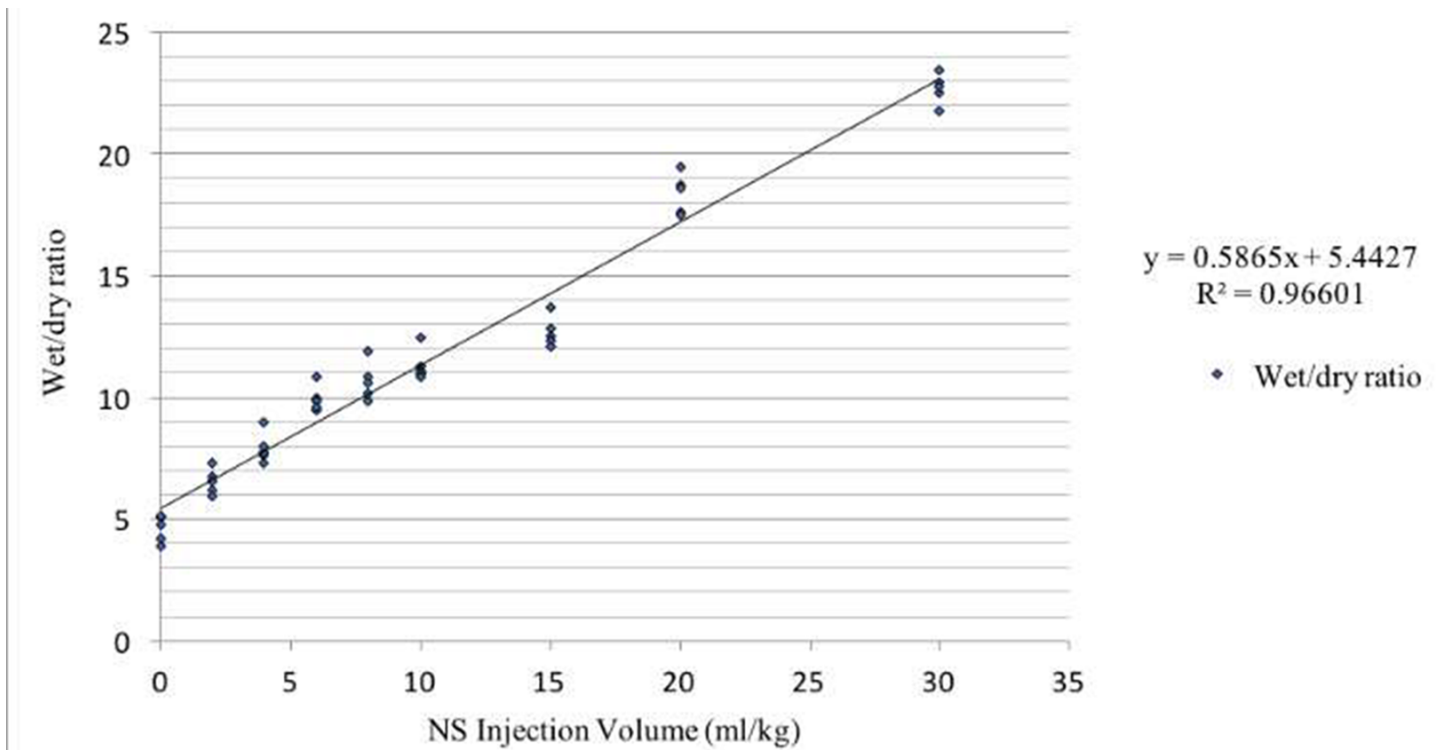


Figure 7

The correlation between NS injection volume and wet/dry ratio in rabbits

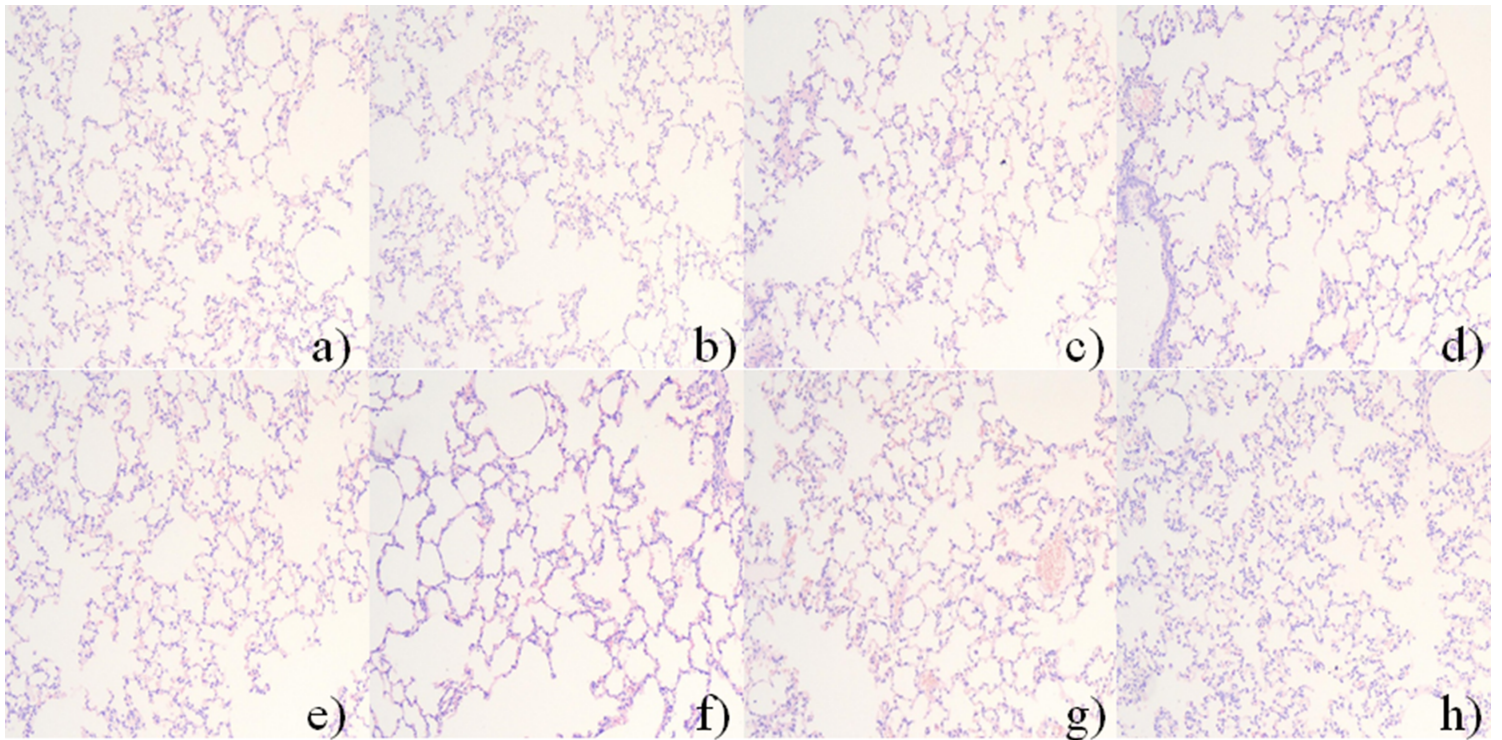


Figure 8

Pathological changes in rabbit lungs after NS injection (*100) : a) injected NS volume: 2 ml/kg; b) injected NS volume: 4 ml/kg; c) injected NS volume: 6 ml/kg; d) injected NS volume: 8 ml/kg; e) injected

NS volume: 10 ml/kg; f) injected NS volume: 15 ml/kg; g) injected NS volume: 20 ml/kg; h) injected NS volume: 30 ml/kg

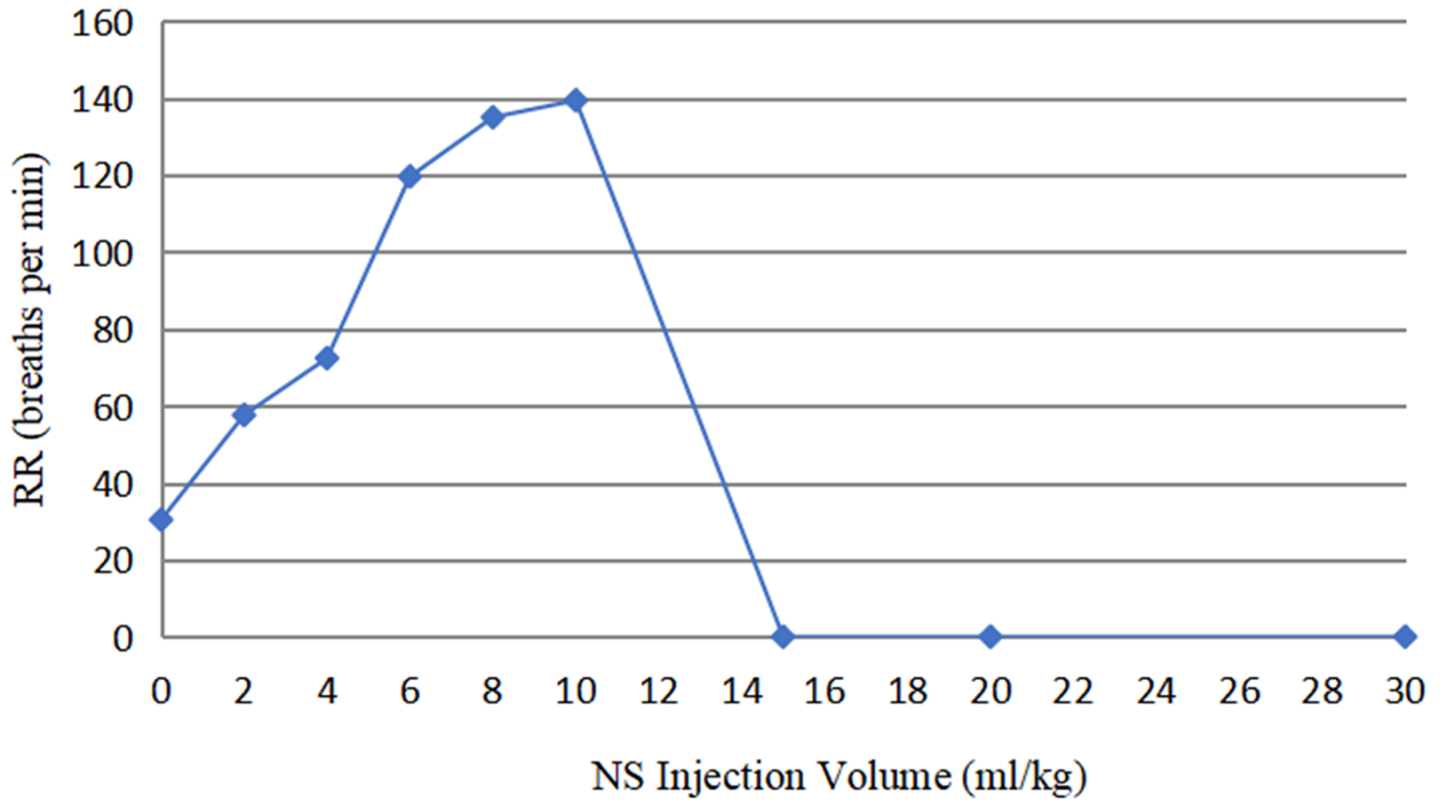


Figure 9

The relationship between NS injection volume and respiratory rate

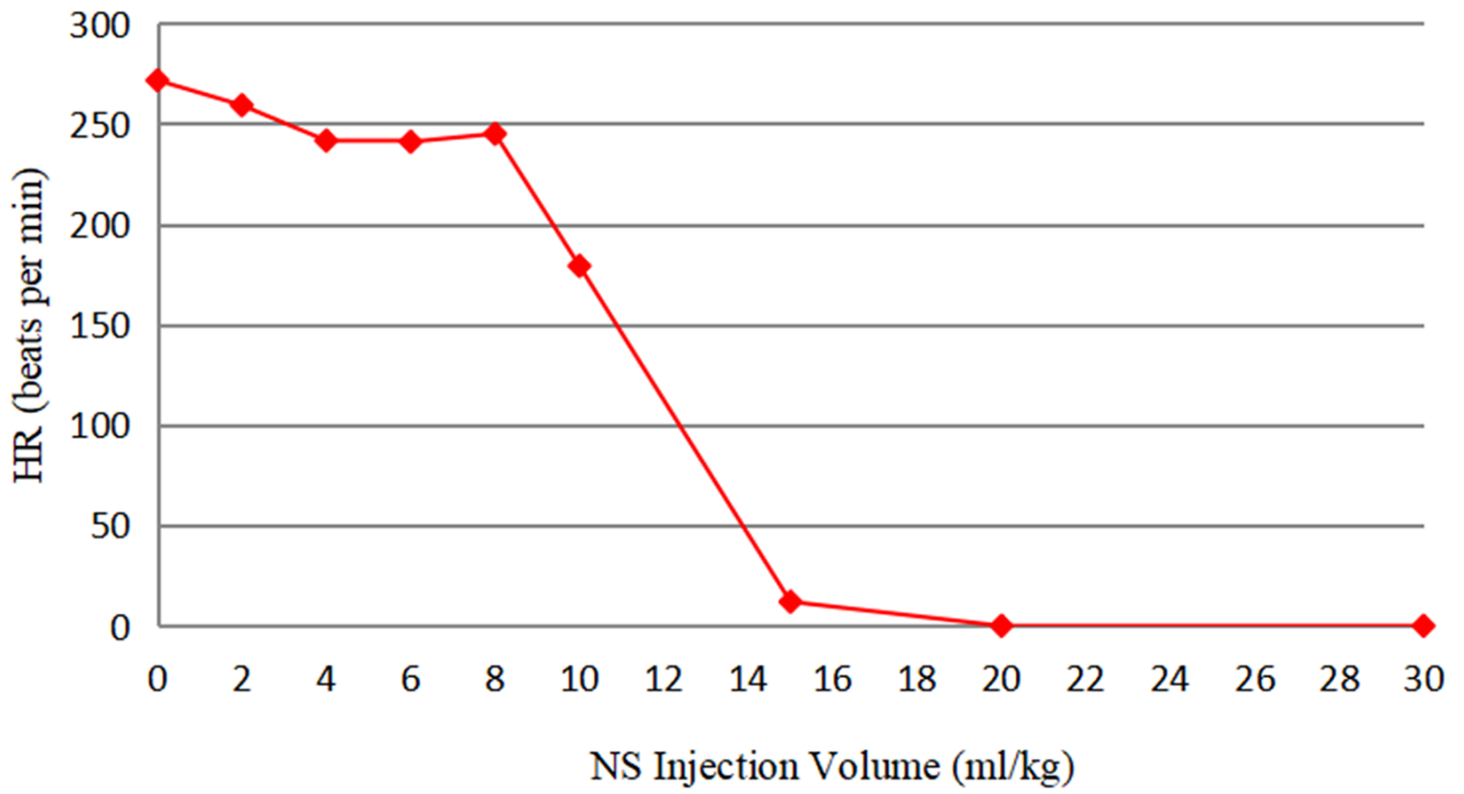


Figure 10

The relationship between NS injection volume and heart rate

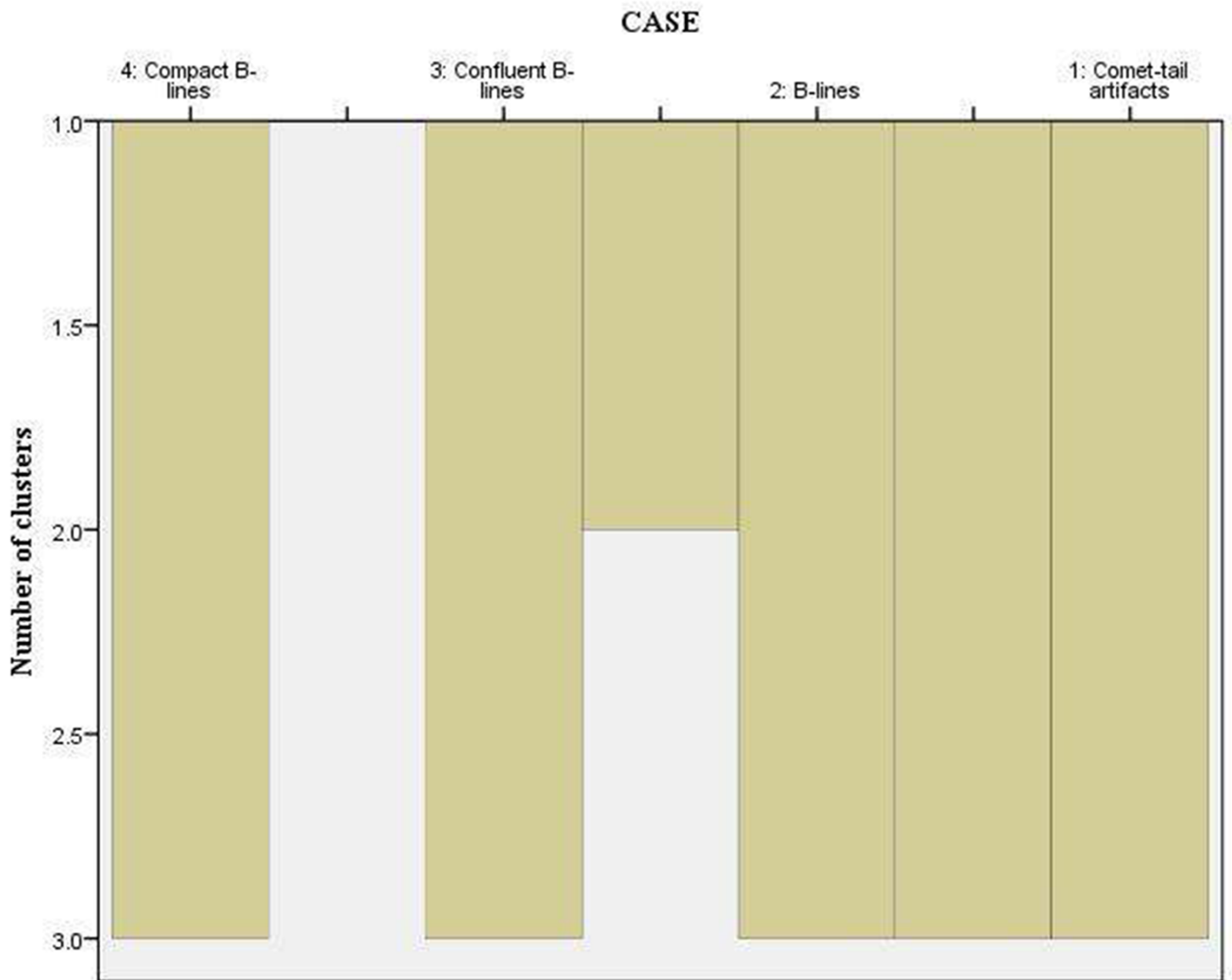


Figure 11

Ice diagram of clustering process for B-lines

Dendrogram using Average Linkage(Between Groups)

Rescaled Distance Cluster Combine

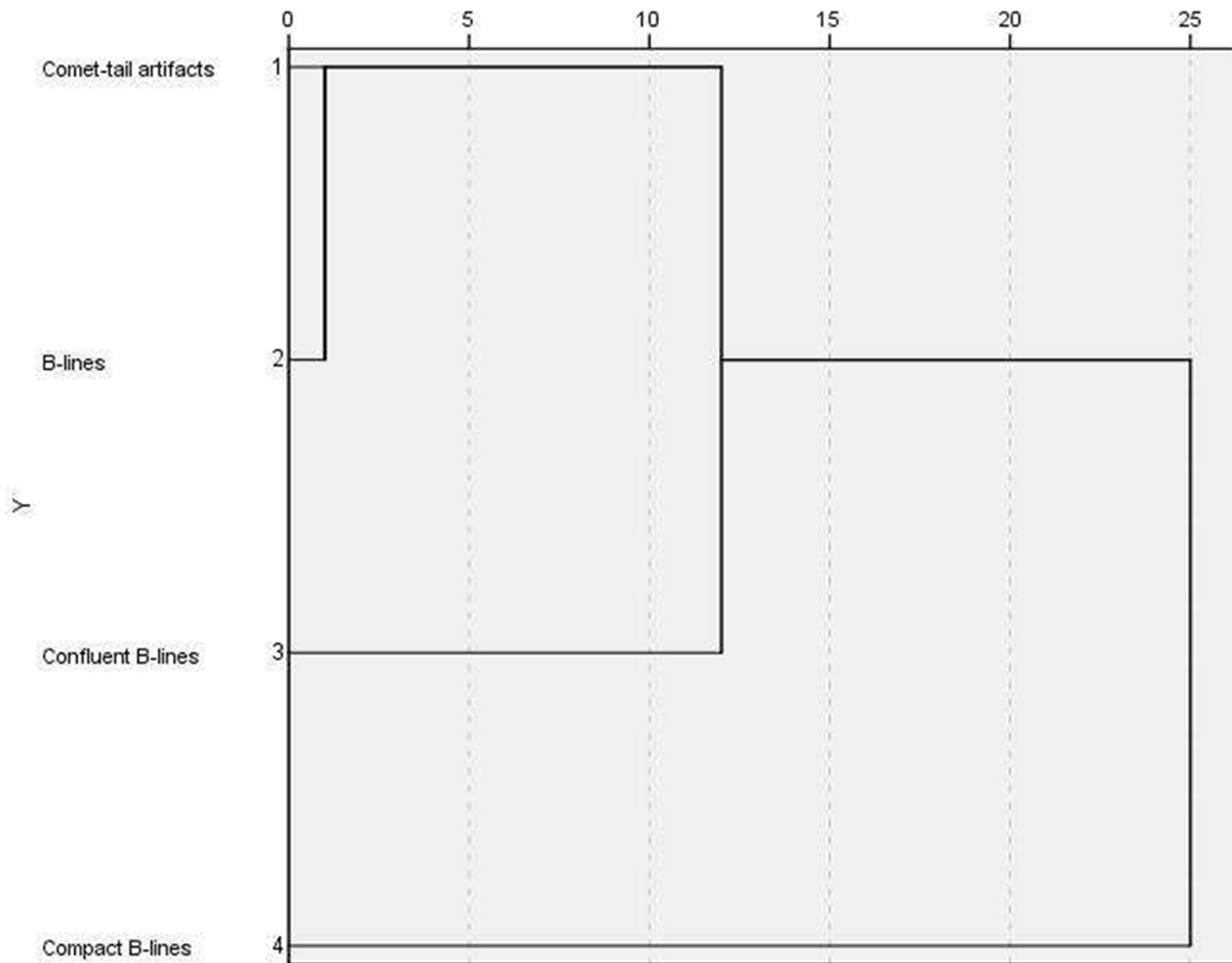


Figure 12

Tree illustrating of clustering process for B-lines

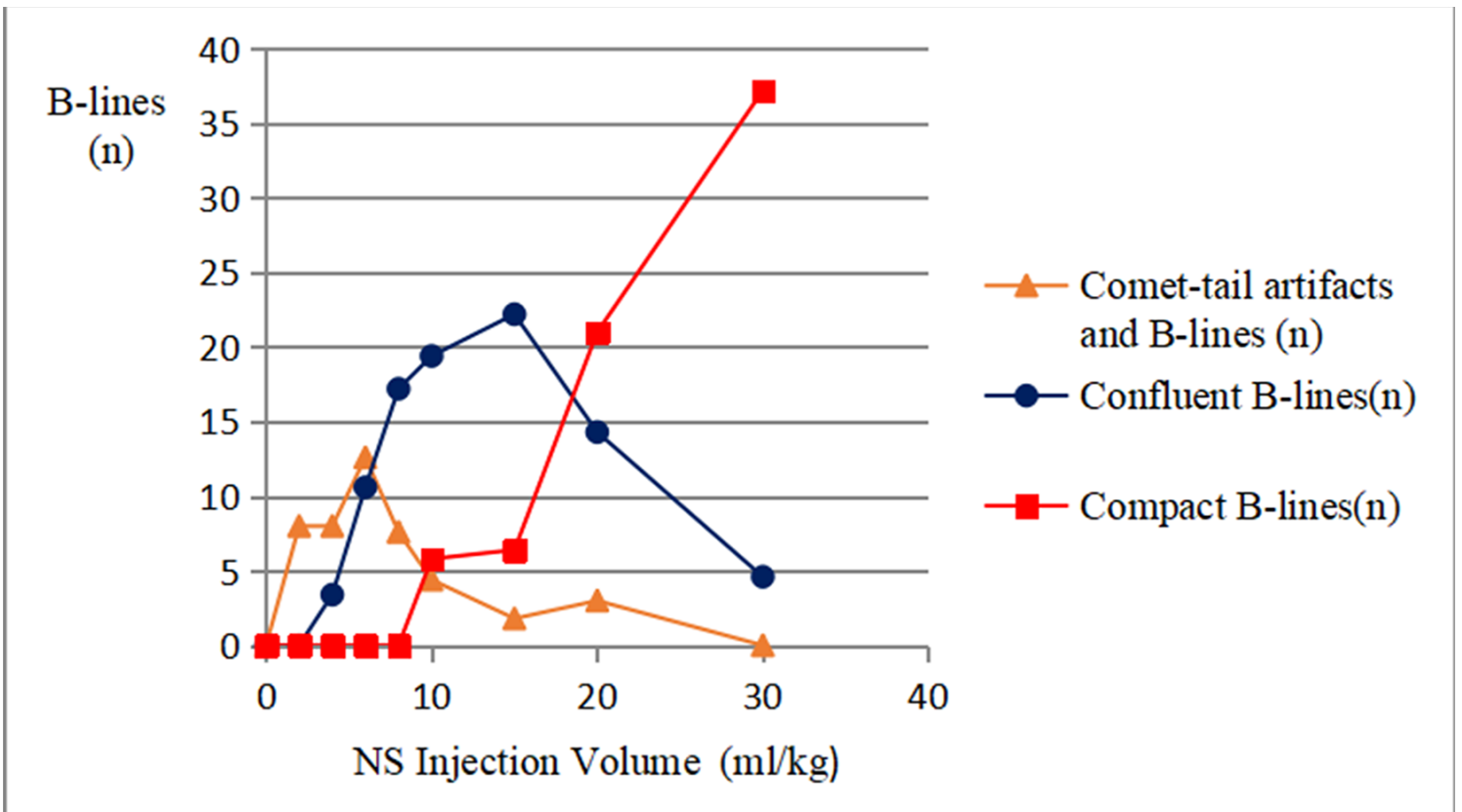


Figure 13

Relationship between NS injection volume and total B-lines

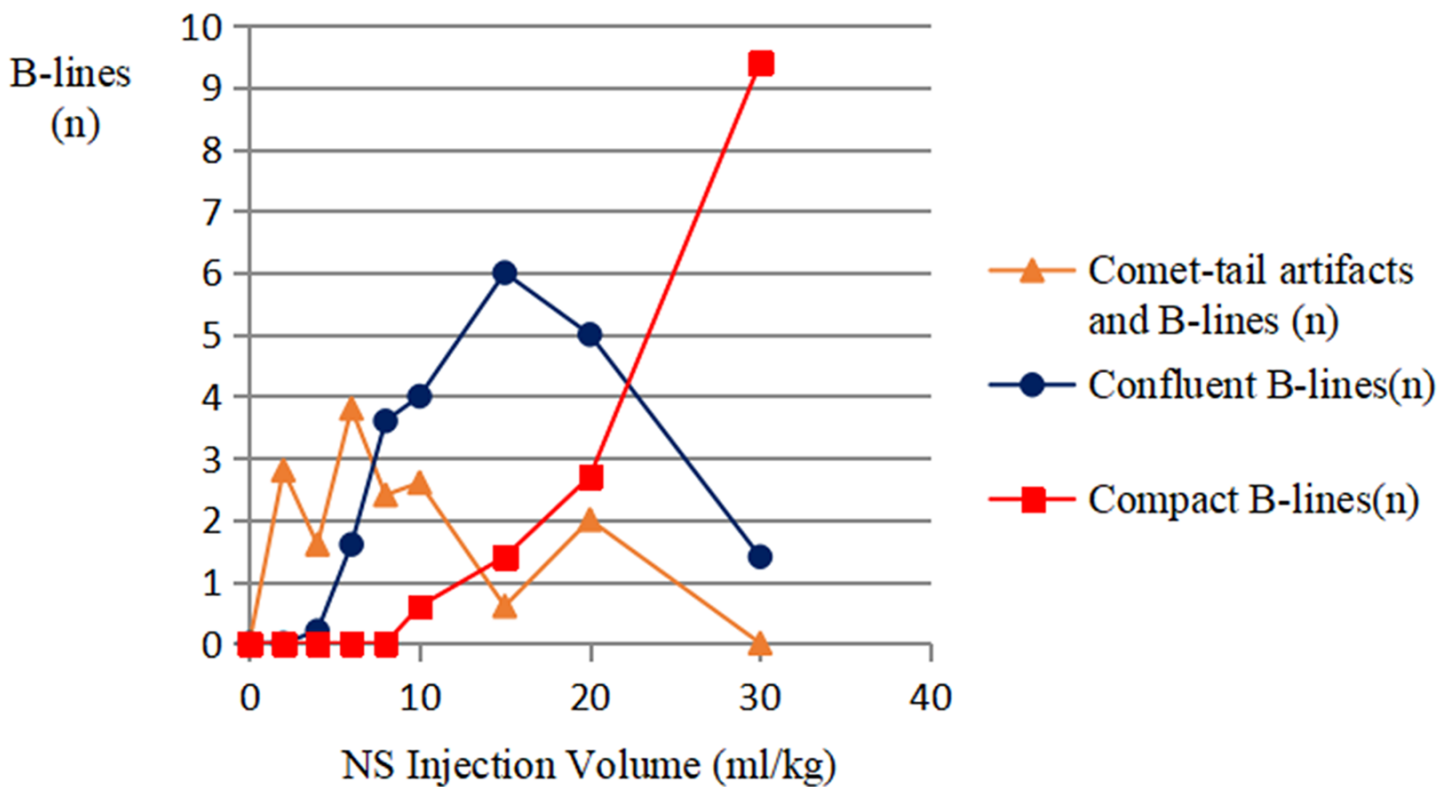


Figure 14

The relationship between NS injection volume and zone 1 B-lines

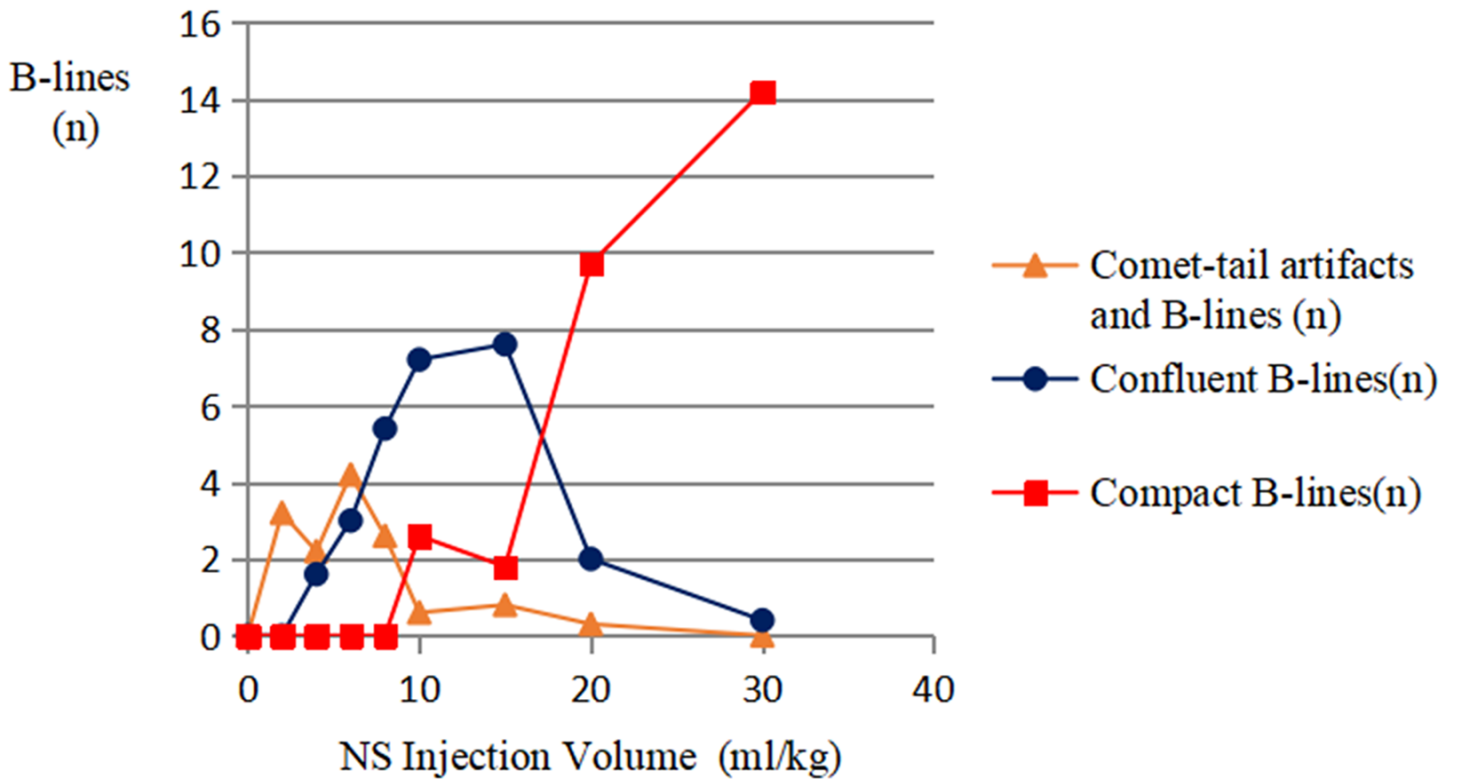


Figure 15

The relationship between NS injection volume and zone 2 B-lines

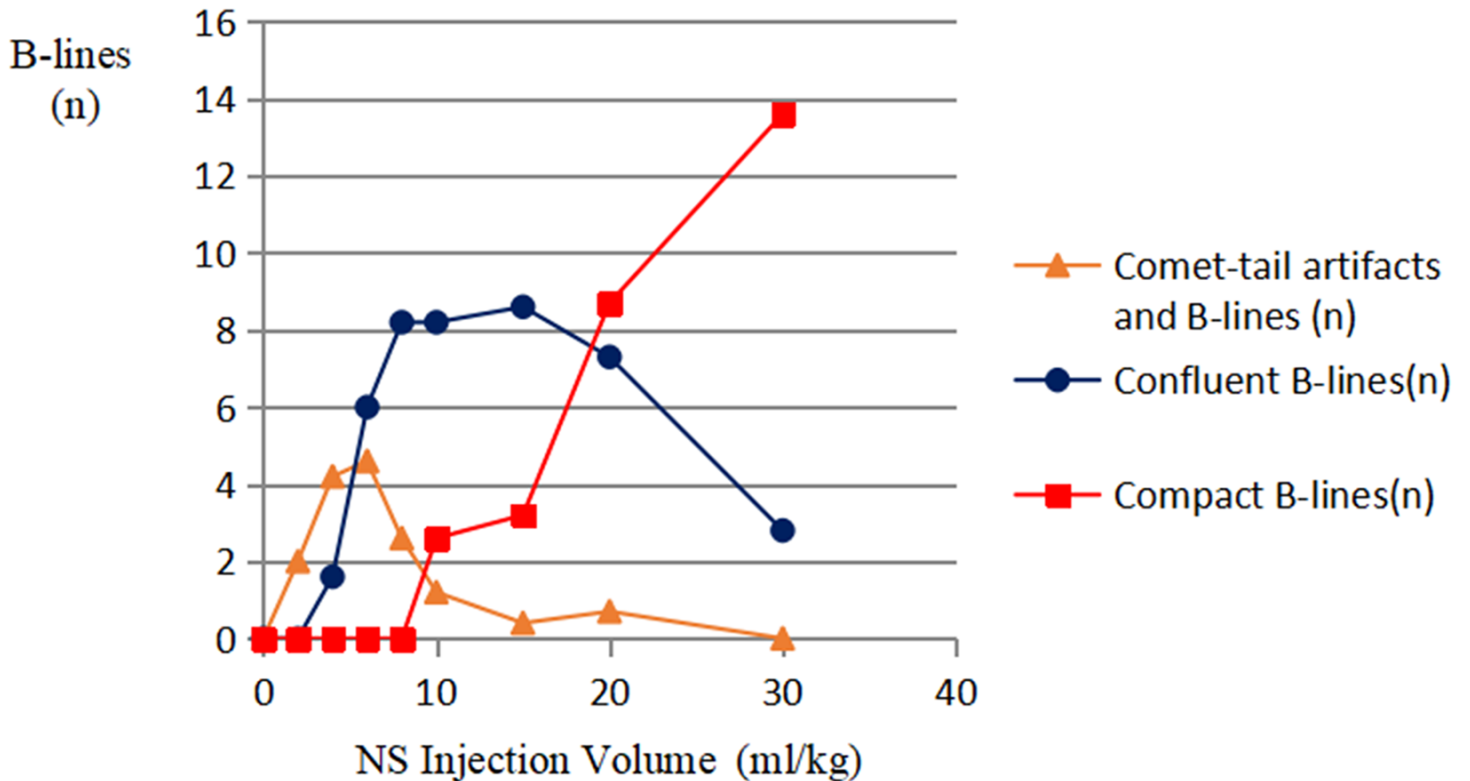


Figure 16

The relationship between NS injection volume and zone 3 B-lines